Fuel 202 (2017) 414–425

Contents lists available at ScienceDirect

Fuel

journal homepage: www.elsevier.com/locate/fuel

Full Length Article

Anti-knock quality of sugar derived levulinic esters and cyclic ethers

Miao Tian [a,*], Robert L. McCormick [b], Jon Luecke [b], Ed de Jong [c], Jan C. van der Waal [c], Gerard P.M. van Klink [c], Michael D. Boot [a,d]

[a] Eindhoven University of Technology, P.O. Box 513, 5600 MB Eindhoven, The Netherlands
[b] National Renewable Energy Laboratory, 15103 Denver West Parkway, Golden, CO 80401, United States
[c] Avantium, Zekeringstraat 29, 1014 BV Amsterdam, The Netherlands
[d] Progression Industry BV, Den Dolech 2, 5612AZ Eindhoven, The Netherlands

HIGHLIGHTS

- Anti-knock quality of four sugar-based cyclic ethers and levulinic esters determined.
- Experiments carried out on both gasoline engine and constant volume chamber.
- Results demonstrate good performance for levulinates and unsaturated cyclic ether.
- Anti-knock behavior qualitatively explained with chemical kinetics considerations.

ARTICLE INFO

Article history:
Received 21 July 2016
Received in revised form 21 November 2016
Accepted 5 April 2017

Keywords:
Sugar
Engine knock
Octane booster
Levulinate
Furan

ABSTRACT

The objective of this paper is to investigate the anti-knock quality of sugar-derived levulinic esters (methyl levulinate (ML) and ethyl levulinate (EL)) and cyclic ethers (furfuryl ethyl ether (FEE) and ethyl tetrahydrofurfuryl ether (ETE)). To this end, combustion experiments were carried out in both an engine and a constant volume autoignition device (modified ignition quality tester (IQT)). The results from both apparatuses demonstrate that ML, EL and FEE have superior anti-knock quality to the reference Euro95 gasoline. ETE, conversely, performed markedly worse than the reference fuel on both setups and might therefore be a more appropriate fuel additive for compression ignition engines. The main reason of the distinctions in anti-knock quality can be found in the molecular structure of the neat biofuels. ML and EL are levulinic esters, with a ketone (C=O) functionality and an ester (C(=O)–O) group on the carbon chain. They can readily produce stable intermediates during the auto-ignition process, thereby slowing down the overall reaction rate. The unsaturated cyclic ether (FEE) has very strong ring C–H bonds. However, the saturated cyclic ether (ETE) has weak ring C–H bonds, which facilitate more readily ring opening reactions. Ethyl side chains on the cyclic ethers further accelerate the reaction rate. Importantly for future research, our results suggest that the modified (IQT) and engine experiments are interchangeable setups with respect to qualitative anti-knock quality evaluation of novel compounds.

1. Introduction

There is a growing demand for transport fuels, particularly in fast-growing countries like China, India and Brazil. This can be seen as an opportunity for new entrants onto the market, most notably biofuels produced in biorefineries. Lignocellulosic biomass makes up the majority of such non-edible feedstocks as corn stover, straw and wood. As the name suggests, lignocellulosic biomass is comprised of (hemi-) cellulose (70–95%) and lignin (5–30%). There are three main (thermo-) chemical routes to convert lignocellulosic biomass into biofuels (Fig. 1):

Abbreviations: ASTM, American society for testing and materials; aTDC, after top dead center; BDE, bond dissociation energy; bTDC, before top dead center; CFR, cooperative fuel research; CN, cetane number; DCN, derived cetane number; EL, ethyl levulinate; EP, ethyl Propionate; ETE, ethyl tetrahydrofurfuryl ether; FEE, furfuryl ethyl ether; ID, auto-ignition delay time; IMEP, indicated mean effective pressure; IQT, ignition quality tester; KI, knock intensity; LHV, lower heating value; MAPO, maximum amplitude of pressure oscillation; MB, methyl butanoate; ML, methyl levulinate; MTHF, methyl tetrahydrofuran; MON, motor octane number; PRF, primary reference fuels; RON, research octane number; SEPO, signal energy of pressure oscillation; SI, spark ignited.

* Corresponding author.
E-mail addresses: m.tian@tue.nl (M. Tian), Robert.McCormick@nrel.gov (R.L. McCormick), Jon.Luecke@nrel.gov (J. Luecke), Ed.deJong@avantium.com (E. de Jong), JanKees.vanderWaal@avantium.com (J.C. van der Waal), Gerard.vanKlink@avantium.com (G.P.M. van Klink), m.d.boot@tue.nl (M.D. Boot).

http://dx.doi.org/10.1016/j.fuel.2017.04.027
0016-2361/

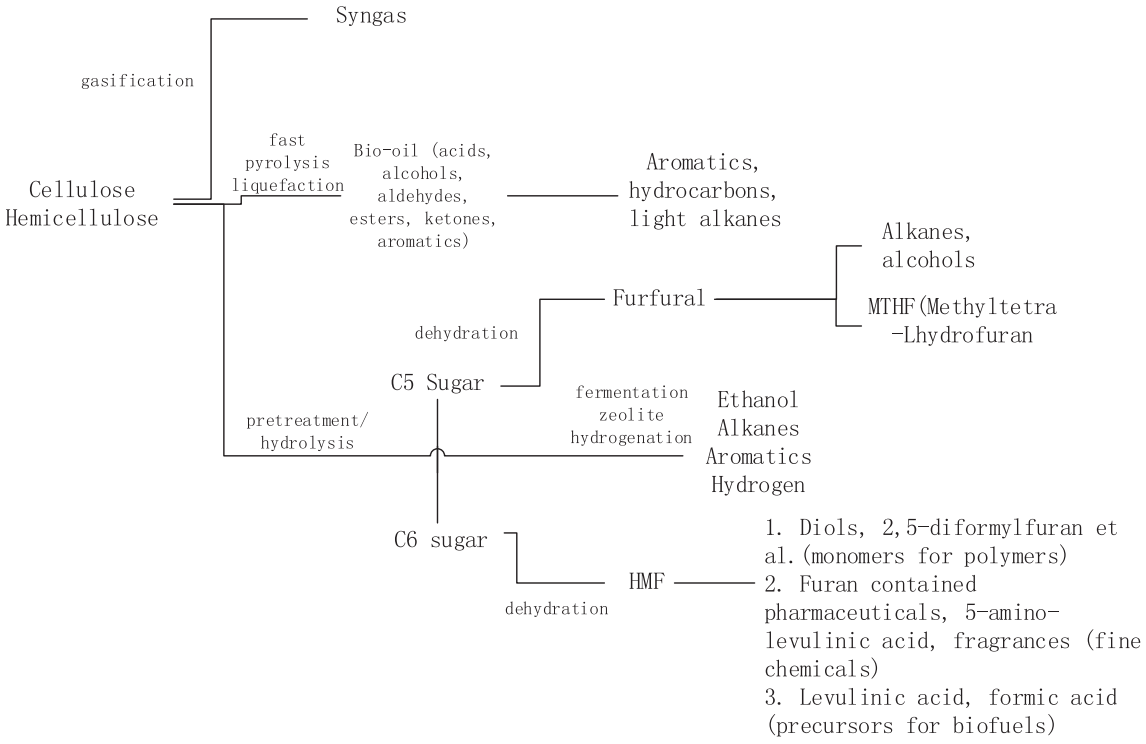

Fig. 1. Possible conversion pathways for (hemi-)cellulose [1,2].

- Gasification → syngas
- Pyrolysis or liquefaction (high temperature) → mixed liquid or solid fuels
- Hydrolysis/dehydration/hydrogenation (lower temperatures) → wide range of (often highly specific) monomers

In the hydrolysis process, C5 and C6 sugars are produced from hemi-cellulose and cellulose, respectively (Fig. 1). These sugars can subsequently react further to produce biofuels investigated in this study: methyl levulinate (ML) and ethyl levulinate (EL), furfuryl ethyl ether (FEE) and ethyl tetrahydrofurfuryl ether (ETE) [3–6] (Fig. 2, Table 1). All selected bio-compounds are either side products or derivatives thereof ([7] for ETE/FEE and [8] for ML/EL) that are formed in the production of 2,5-furandicarboxylic acid (FDCA), a building block for renewable polyesters [9], from sugar. When FDCA is successfully used, the potential of using levulinate as well as furan derivatives for fuel applications is highly relevant.

Furfuryl ethyl ether (FEE) and ethyl tetrahydrofurfuryl ether (ETE) have reportedly the potential to curb soot emissions in compression ignition engines [7]. Similar tests conducted for EL showed an equally promising soot reduction potential [10]. ML and EL have a very low derived cetane number (DCN) (<10) [10]. Considering the inversely linear relationship between cetane number (CN) and research octane number (RON) [11], both levulinic fuels are expected to have a high RON and might therefore be attractive candidates for use as bio-octane boosters in spark-ignition (SI) engines [12].

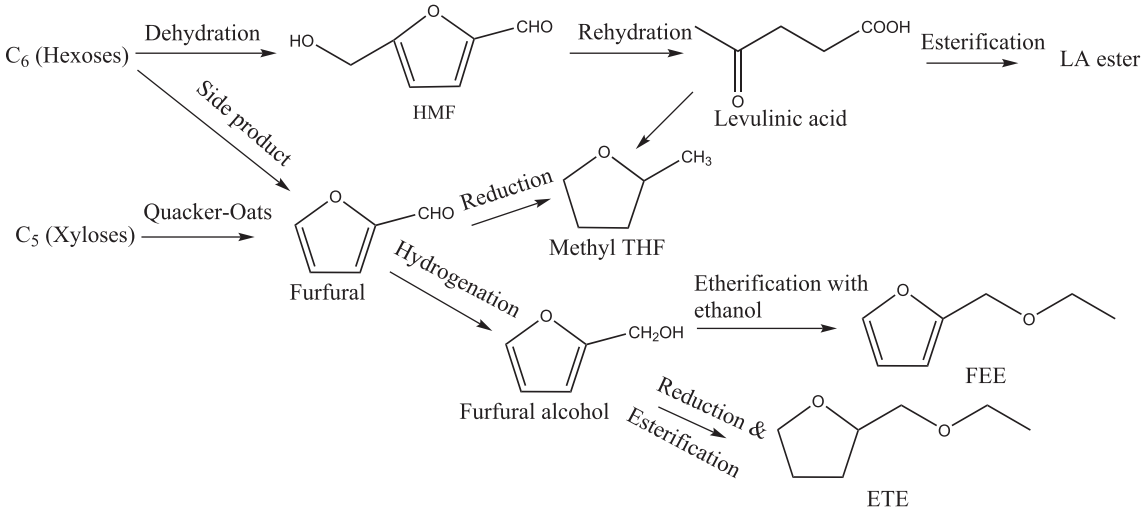

Fig. 2. Production routes of the investigated compounds [2,5,6].

Table 1
Physiochemical properties of the neat biofuels.

Fuel	Formula	Density g/L	BP[a] °C	Viscosity cP at 25 °C	LHV MJ/kg	LHV MJ/L	DCN[b]	$\Delta H_{vaporization}$ KJ/kg at 25 °C
ML	$C_6H_{10}O_3$	1.051[a]	194	1.93 [14]	22.38	23.5 [12]	7.8	332.5 [12]
EL	$C_7H_{12}O_3$	1.016[a]	204	2.0 [12]	24.3	24.8 [12]	6	306.7 [12]
FEE	$C_7H_{10}O_2$	0.9935[c]	150	0.95 [7]	28.80	30.5 [7]	18.4	–
ETE	$C_7H_{14}O_2$	0.9396[c]	156	0.91 [7]	30.70	30.8 [7]	78.9	–

[a] BP: boiling point. Data retrieved from MSDS, the densities of ML and EL are at 20 °C.
[b] Measured in this study.
[c] From [7] at 15 °C.

In order to test the potential of aforementioned compounds as octane boosters, the anti-knock quality of the neat oxygenates blended with gasoline, was evaluated in an SI engine, and ignition delay times were measured over a range of temperature in a modified ignition quality tester (IQT). Experimental results will subsequently be discussed with the aid of qualitative chemical kinetics considerations.

2. Methodology

2.1. Fuels

Molecular structures of the neat biofuels are shown in Fig. 3. Physicochemical properties of the neat and blended (e.g., to 10 vol.-% in commercial Euro95 gasoline) biofuels are listed in Table 1 and 2, respectively. Of particular interest here are the unexpectedly high DCN (78.9) for ethyl tetrahydrofurfuryl ether (ETE) and low volatility of methyl (ML)- and ethyl levulinate (EL) relative to the distillation T90 (190 °C) and endpoint (225 °C) limits for gasoline. The high boiling point may cause poor mixture distribution in the intake manifold and combustion chambers, or lead to high levels of lube oil dilution. The heat of vaporization of ML and EL (332.5 and 306.7 kJ/kg) are similar to gasoline (298 kJ/kg [13]). Heats of vaporization have not been reported for FEE and ETE, but should be in a similar range given the lack of highly polar alcohol functionality.

Furthermore, on a volumetric scale, ETE and FEE have very similar lower heating values (LHV) compared to gasoline, because of their density differences, while ML and EL score considerably lower on this point with ML having only a slightly higher volumetric LHV than ethanol (23.4 MJ/L).

To analyze the composition of the reference gasoline fuel, a detailed hydrocarbon analysis was conducted in accordance with the ASTM D6729 guideline. The results, summarized in Table 3, revealed a relatively high aromatic content of 31.58%, as well as the presence of commonly blended oxygenates: methanol, ethanol and methyl tert-butyl ether (MTBE) (0.4%, 3.9%, 3.1% by volume, respectively).

2.2. Engine

Engine experiments were conducted on a Volvo T5 turbocharged port fuel injected 5-cylinder SI engine. A schematic overview of the setup is shown in Fig. 4 and the engine specifications can be found in Table 4. In light of the fact that SI engines tend to be more knock prone at low speeds, 1500 RPM is selected as the reference point in this study. Earlier work [15] has shown that the anti-knock quality of various fuels is quite similar at part-load and full-load. Accordingly, only the full load or wide open throttle (WOT) case is considered here.

Engine-out coolant and oil temperatures are kept constant at 91 °C. The setup is equipped with a water-cooled Schenck E2-330 eddy current brake. A Kistler piezoelectric pressure sensor with a resolution of 3600 samples per revolution is installed onto one of the cylinders. Intake pressure is set to 1.26–1.28 bar (abs.) and a constant intake temperature of 20 ° C is maintained. The default spark timing for the neat gasoline reference fuel is 12 crank angle degrees before top dead center (° CA bTDC). Each fuel is subjected to a spark timing sweep, whereby 200 cycles are recorded and used to calculate the IMEP, efficiency and other engine parameters for each cycles, the standard deviation were calculated and shown as error bars in the engine performance results. The day-to-day variations were also calculated for Euro95 (3 different days) by using the averaged pressure of the 200 cycles for each working point. Limited by the amount of fuels purchased, the other fuels have only tested in one day, so no day-to-day variation is shown here.

There are several in-cylinder pressure-based parameters that can be used to evaluate the degree of knock, including the 1st

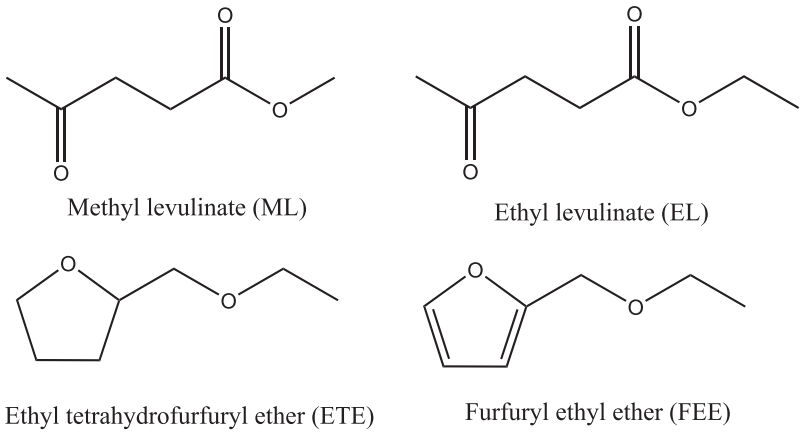

Fig. 3. Neat biofuel molecular structures.

Table 2
Physiochemical properties of the blends.

Fuel	Density g/L	Oxygen content [wt.-%]	LHV MJ/kg	LHV MJ/L
Euro95	0.74	2.24	41.91	31.01
10% ML	0.77	5.8	39.2	30.3
10% EL	0.77	5.4	39.6	30.4
10% FEE	0.77	4.5	40.5	31.0
10% ETE	0.76	4.3	40.8	31.0

Table 3
Components of Euro95.

Component	vol.-%
Paraffin	48.90
Aromatics	31.58
Olefins	6.62
Oxygentates	7.44
Naphthenes	4.60
Others	0.86
Empirical formula	$C_{6.11}H_{11.51}O_{0.12}$

and 3rd derivative of the pressure, peak pressure, rate of heat release and band pass filtered pressure [16,17]. Analysis of the latter parameter is the most widely adopted method in engine knock studies [16].

In this study, the signal energy of pressure oscillation (SEPO), which is the signal energy of the band pass filtered pressure over a certain knock window is used to determine the knock intensity (KI), whereby the pressure signal is filtered by a 6–25 kHz band pass filter from 10 to 40° CA after top dead center (aTDC). The KI threshold is defined by the sharp increase of SEPO that occurs at a different crank angle for different fuels as the spark timing is advanced. In this study, knock limited spark advance (KLSA) is defined as the spark timing at which KI surpasses 1.2 pa^2 s.

For a given set of operating conditions and engine specifications, a more advanced spark timing at the KLSA is indicative of a better anti-knock quality fuel, typically yielding a combination of improved torque, thermal efficiency and fuel economy.

Fuel conversion efficiency is used in this study and calculated by Eq. (1), wherein P is power, m is the mass of injected fuel per cycle.

$$\eta_f = \frac{P}{LHV \times m} \quad (1)$$

2.3. Constant volume autoignition device

A modified ignition quality tester (IQT) was used to measure the auto-ignition delay time (ID) of a test fuel as a function of temperature and pressure. Detailed description of the setup can be found in [18]. While the chamber charge is initially heterogeneous in nature, homogeneous conditions may nevertheless be assumed given ample mixing time (e.g., ID >40 ms [19]). Under such conditions, chemical kinetic effects far outweigh the effects of mixing.

In this study, temperature sweeps were conducted at a constant pressure of 10 bar and stoichiometric air/fuel ratio. To this end, the IQT chamber is pressurized to 10 bar with synthetic air, comprising 21% O_2 in N_2, at the reaction temperature within the 700–950 K window of interest.

3. Results and discussion

3.1. Engine

3.1.1. Knock limited spark advance

Fig. 5 shows SEPO as a function of spark timing. Irrespective of fuel, advancement of the timing always manifests in a higher SEPO. For most oxygenated blends, the knock limit, demarcated here by the dashed line, is breached at significantly earlier timings than is the case for neat gasoline. The sole exception is the ETE blend that, as might have been predicted based on the high DCN of the neat biofuel (Table 1), is considerably more reactive than the reference fuel. Blends with the levulinic esters show the best performance, with 10% FEE trailing not far behind.

The KLSA of the blends (Fig. 5) would thus appear to correlate quite well with the DCN of neat oxygenate (Table 1). Accordingly, the data suggests that relative anti-knock quality in an engine can be predicted by comparatively low-cost and less fuel demanding IQT experiments, consistent with the inverse correlation between RON and DCN [11] and other recent findings [20].

3.1.2. Load, efficiency and fuel economy

Engine performance, represented by the indicated mean effective pressure (IMEP), fuel conversion efficiency and volumetric indicated specific fuel consumption (ISFC), is evaluated only at the KLSA and is summarized in Table 5. Volumetric fuel consumption is studied here because it is deemed more relevant for practical purposes than the gravimetric variety. Detailed engine performance data, covering the entire spark timing sweep can be found in the Appendix A.

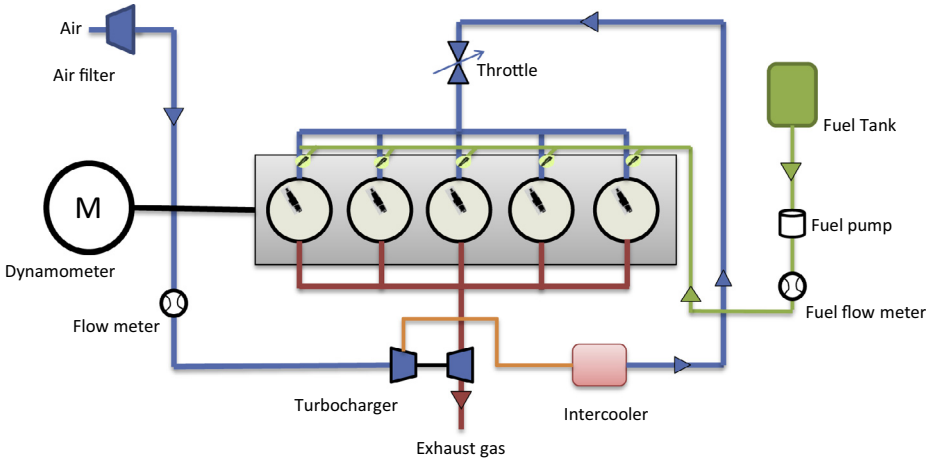

Fig. 4. Schematic representation of the test engine.

Table 4
Engine specifications.

Engine	2.5T (B5254T6)
Type	In-line 5-cylinder LPT
Displacement [cm^3]	2521
Bore [mm]	83
Stroke [mm]	93.2
Combustion chamber type	Pent-roof
Compression ratio [–]	9.0:1
Valves per cylinder	4
Ignition sequence	1-2-4-5-3
Fuel, octane requirement [RON]	95-98
Max output, [kW(HP) @ RPM]	147(200) @ 4800
Max torque, [Nm @ RPM]	300 @ 1500-4500
Maximum boost pressure [bar]	1.38

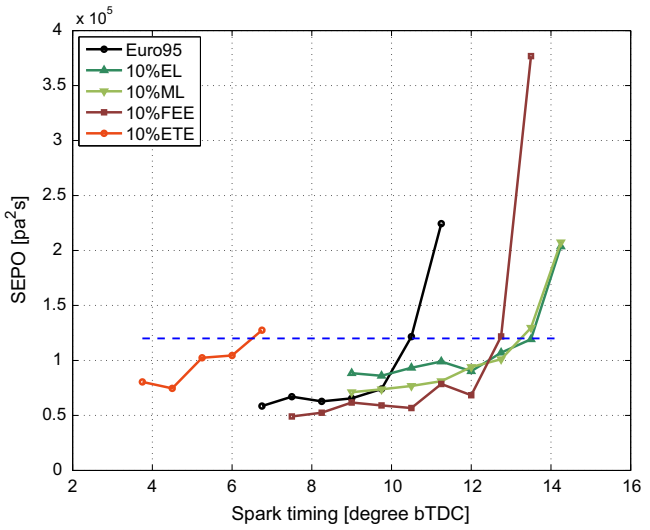

Fig. 5. SEPO as a function of spark timing for all fuels at WOT and 1500 RPM.

With respect to the reference fuel, an earlier and later KLSA generally translates into modest gains and penalties in IMEP and fuel conversion efficiency, respectively. There is one notable exception, however, that requires further investigation. It would appear that the blend with the most advanced KLSA, i.e. 10%EL, performs similar in terms of IMEP and efficiency compared to the reference fuel.

Pertaining to fuel economy, it can be seen that the energy density penalty otherwise incurred by the presence of oxygen in the additives can be partially to fully offset by a combination of higher mass densities (Tables 1 and 2) and improvements in thermal efficiency.

Combustion phasing is expressed here as the cycle averaged CA50, it is the crank angle at which 50% of the total heat release occurs (Fig. 6). For a given spark timing and considering the margin of error, the differences in CA50 is negligible for all the fuels save for the ETE blend.

3.2. Chemical group additivity analysis

The anti-knock quality results from engine experiments are consistent with their DCN, i.e., the lower DCN the better knock resistance quality. Many physical and chemical properties can be predicted based on the molecular structure, and in particular the group additivity principle has been used to predict fuel ignition properties, such as cetane and [21–23] octane number [24,25]. Recently, oxygenates are also considered in this prediction model for auto-ignition delay times [26].

In order to investigate the impact of oxygen functionalities, multiple linear regression is used to study the relationship between DCN and molecular structure. The DCN of 47 pure compounds comprising five chemical classes (i.e., paraffin, cycloparaffin, ketone, ester, ether) are obtained from literature as the training data. The functional groups considered here are: CH_2, CH_3, CH, ether (COC), ketone (C=O), ester (C(O)O), furan, cyclic.

The results of the regression analysis can be written as below (Eq. 2). The regression coefficient (R^2) is 0.945. N_x is the number of functional group x in the compound. Aldehyde and highly branched ether groups were not considered as there is little data in literature. Moreover, these are not functionalities that were tested in this study. The CH_2 and COC functional groups in furan rings were not counted twice as N_{CH_2} or N_{COC}, but were captured in the regression as a furan group. Tetrahydrofurans are considered to be cyclic rings analogous to cycloparaffins.

This model was validated by using ten compounds obtained from literature. As shown in Fig. 7, there is a good match between the real DCN data and the predicted values)R^2 = 0.94). Furthermore, the equation also qualitatively shows the correct impact of each functional groups with respect to the DCN. CH and oxygenated groups (i.e., ketone, ester), and cyclization in general, all have a negative impact on DCN and a commensurately higher anti-knock quality. Conversely, ether, CH_2 and CH_3 groups have positive impact on DCN and lower the aforementioned quality.

$$DCN = 1.1082 + 5.9172N_{CH_2} + 8.0518N_{CH_3} - 1.8774N_{CH} + 20.356N_{COC} - 9.6051N_{C=O} - 17.28N_{C(O)O} - 15.629N_{cyclic} - 10.3N_{furan} \quad (2)$$

3.3. Constant volume autoignition device

Engine experiments have shown that ML, EL and FEE have a superior anti-knock quality than the reference Euro95 gasoline. The knock resistance of a fuel is dominated by its auto-ignition chemistry at certain temperature and pressure. Accordingly, it is expected that these fuels have a commensurately longer ID when measured under engine-like conditions. To validate this assumption, auto-ignition behavior was evaluated in a modified IQT setup, which is a constant volume autoignition device.

Fig. 8 shows the ID of neat ML, EL, FEE and ETE as a function of temperature (626–1000 K) at 10 bar, and data for iso-octane reported by Bogin et al. [28] as a comparison. No negative temperature coefficient (NTC) behavior is observed for the oxygenates, whereas iso-octane shows quite clear NTC behavior as expected. ML and EL have similar ID as iso-octane (RON = 100) for temperature above 870 K, but show longer ID at lower temperatures because of the well-known low temperature autoignition route available to long chain alkanes. FEE has lower ID than iso-octane when temperature (T) above 820 K, but longer ID at lower temperatures. When T > 865 K, the ID of FEE is shorter than 40 ms, so that the chamber cannot be assumed homogeneous. ETE shows much a shorter ID than iso-octane at all temperatures. The results are in line with expectations in so far as the ranking amongst the fuels is equal to that established earlier in the engine section (Fig. 5 and Table 5). However, the ML and EL results are more ambiguous. This may be due to their high boiling point, which might prevent proper vaporization, causing the fuel to impinge on the IQT chamber wall.

3.4. Chemical kinetics analysis

Levulinic esters have a ketone and an ester functionality on the carbon chain, while FEE and ETE both contain two ether groups in their structure. These structural factors will have a significant

Table 5
Engine performance at the KLSA.

Fuel	KLSA [°CA bTDC]	IMEP [bar]	Thermal eff. [%]	CA50 [°CA[a]TDC]	Vol. ISFC [ml/kW h]
Gasoline	10.5	14.2	37.1	18.5	312.9
10% EL	13.5	14.2	37.2	17.2	317.5
10% ML	13.3	14.5	38	16.4	313.6
10% FEE	12.7	14.4	37.9	16.9	310.9
10% ETE	6.5	13.4	35.1	25.9	333.3

[a] All values in this table are taken at the knock limited (KL) spark timing by means of linear interpolation of two nearby spark timings.

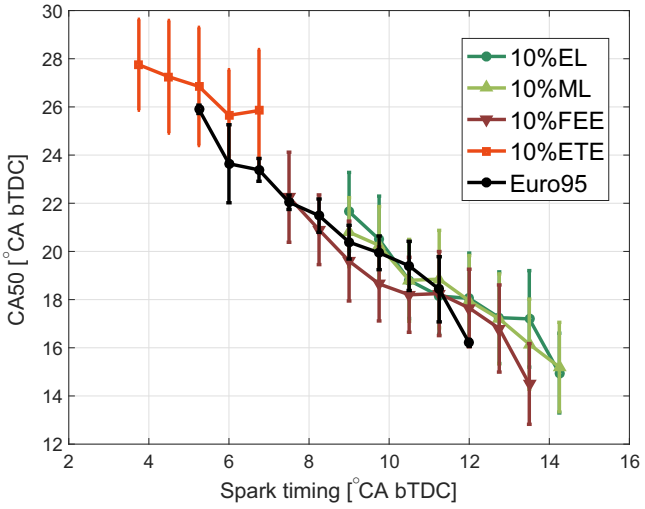

Fig. 6. CA50 as a function of spark timing for all fuels at WOT and 1500 RPM.

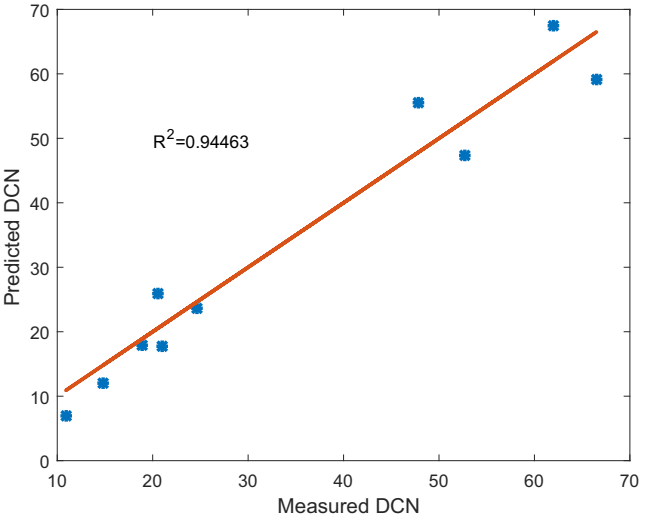

Fig. 7. Comparison of measured and predicted DCN (Data obtained from [11,27]).

impact on autoignition kinetic mechanisms as investigated in this section.

3.4.1. Levulinic esters

Thion et al. [29] conducted a computational study on ML oxidation kinetics. Apart from this study, very little has been published on the kinetics of levulinate compounds. As a consequence, the oxidation mechanism of methyl butanoate (MB) will be used as a proxy. MB has similar structure as ML, except that ML has a carbonyl group (C=O) attached at the C_4 position. MB has a very

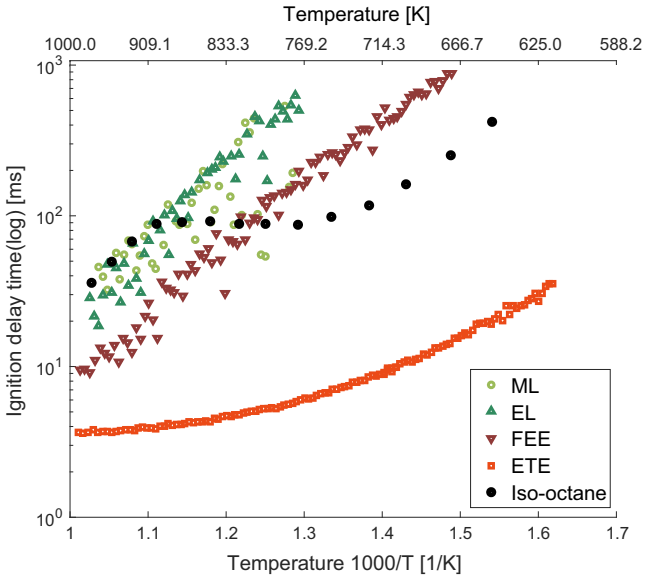

Fig. 8. Ignition delay time as a function of temperature for all fuels at 10 bar, with iso-octane as a reference from Bogin et al. [28].

low DCN as well (6 [11]) and its autoignition mechanism has been subject of several studies [30–35].

Using the kinetic model from Hakka et al. [35], the fuel radicals can react via three pathways (Fig. 9), a) O_2 addition reactions producing alkyl peroxy radicals (ROO), which are important for most alkanes; b) β-scission reactions; c) reaction with O_2, yielding α,β-unsaturated ester and HO_2. In other mechanisms, such as Gail et al. [30] and Dooley et al. [31], reactions with RO_2 or HO_2, producing alkoxy fuel radicals are also considered. This pathway is quite important in the mechanism of butanone developed by Burke et al. [36]. ROO radicals can either undergo isomerization reactions producing alkylhydroperoxy radicals (QOOH) or react via concerted elimination reactions to produce unsaturated esters. QOOH radicals can subsequently undergo β-scission, cyclization or subsequent O_2 addition reactions. The latter reaction, followed by low temperature branching reactions.

Several C–H and C–C bond dissociation energies (BDE) of MB are shown in Fig. 10 [33]. It can be seen that due to the attraction from the O atom, the C–O bond is stronger than the C–C bond and the $C_\beta - H$ bond (C2 in Fig. 11) is relatively weak (93.6 kcal/mol compared to 98.5 kcal/mol on the $C_\gamma - H$) because of the C=O bond, making this site the most preferred place for initial radical formation reactions and the following H atom abstraction reactions. Normally, for alkanes, the dominant pathway in the low and intermediate temperature regime will be O_2 addition reactions and the following low temperature branching reactions. However, because of the carbonyl bond (C=O), fuel radicals, particularly at the C atom adjacent to C=O bond, the fuel radicals will be largely consumed by reaction b) and c), producing stable unsaturated

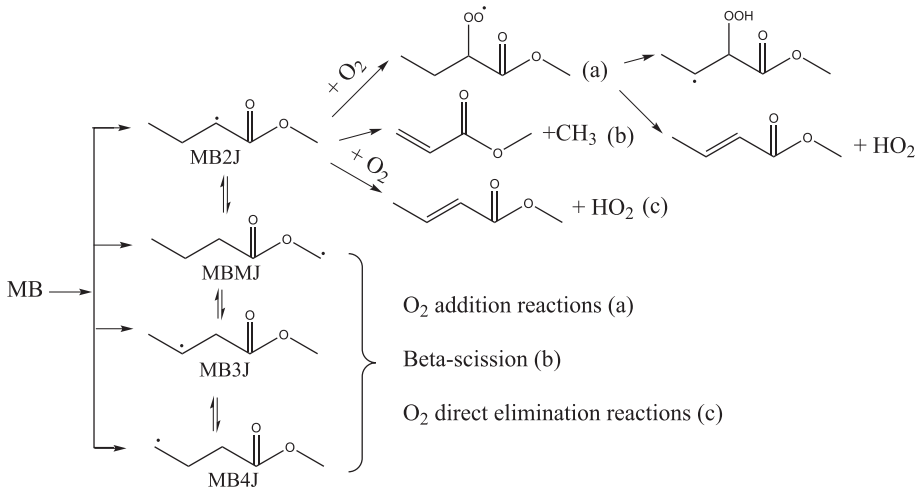

Fig. 9. Simplified reaction scheme of methyl butanoate [35].

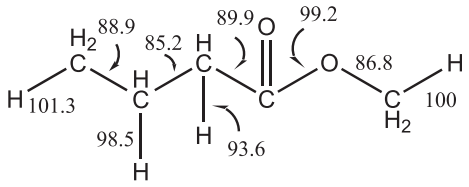

Fig. 10. Bond dissociation energies in methyl butanoate (unit: kcal/mol) [33].

esters and small radicals. Moreover, $C_2H_5CHC(O)OCH_3$ radicals are resonance stable (Fig. 11). The change in dominant reaction pathway and production of stable intermediates slows down the overall reaction rate, particularly in the low temperature range.

Compared to MB, ML has one more carbonyl group on the chain to impact the nearby C–H bond, so that C_2, C_3 and C_5 are all impacted by the carbonyl group. It has the same amount of H atoms available for H atom abstractions as does MB and the BDE of the adjacent C–H bond is also weakened by the carbonyl atom. ML has the same number of C atoms as methyl pentanoate, their DCN are 7.8 (Table 1 and 13.3 [11], respectively, which indicates that adding a ketone functionality will make the compound more stable. Thion et al. [29] showed that in ML reaction kinetics, the sites between the two functional groups (C_3 and C_4) are the most favorable sites for H atom abstraction reactions. The produced fuel radicals are resonance stabilized as well. Similar to MB, O_2 addition reactions and the following low temperature branching reactions are not the dominant routes. Rather, direct O_2 direct and β-scission are also competitive. The possible simplified reaction scheme of ML is shown in Fig. 12.

EL has one more methylene (CH2) group on the ester side compared to ML. It is slightly more stable than ML from the DCN data, while from the engine tests, their anti-knock quality are very similar. The IDs from modified IQT also show very similar data. This indicates that the two oxygen functional groups (C=O and C–O–C) are the dominant factor to impact the ignition delay times compared to the chain length.

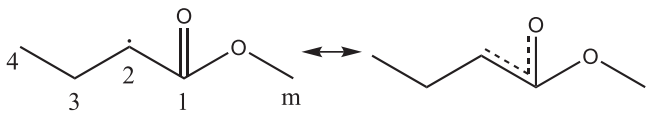

Fig. 11. Resonance stable structure of $C_2H_5CHC(O)OCH_3$ [31].

As MB can be used as a proxy for ML, so too can ethyl butanoate (EB) serve this purpose for EL. Compared to MB, a reaction unique to EB is molecular elimination, producing ethylene and butanoic acid [35]. This reaction occurs more readily for an ethyl ester, because the transition state for this reaction is a six-membered ring (Fig. 13), which has relatively low energy barrier [37]. The discrepancy in ID amongst EB and MB increases with temperature [35].

3.4.2. Furan and tetrahydrofuran ethers

Furans generally have strong C–H bonds on the ring (higher than the ring C–H bond in toluene, shown in Fig. 14) [38], rendering these heterocyclic structures particularly stable. However, their side chain C–H bonds are weaker than in toluene. 2-Methylfuran (2-MF) has a weaker C-H BDE for the methyl C-H when compared to toluene. Furan, 2-MF and toluene are all very stable, and have a small CN (7, 8.9 and 3, respectively [39,11]).

No reaction mechanism could be found for FEE or ETE in literature, and in order to qualitatively analyze the oxidation pathways of these two compounds, the mechanism of 2-MF and 2-methyl tetrahydrofuran (2-MTHF) are studied instead. In addition, 2-MF has shown some promise as a neat fuel for spark ignition engines [42,43].

The majority of 2-MF is consumed by H atom ipso addition and H atom abstraction reactions taking place on the alkyl side chain, producing furan and 2-furanyl methyl radicals, respectively (Fig. 15). The main reasons for the overall slow reaction rate of 2-MF are: the stable furan ring structure and resonance stabilized intermediates, such as 2-furanyl methyl radicals, combined with the lack of low temperature branching reactions.

In FEE, conversely, which has an ethyl ether functionality connected to the methyl side group, the C_α-H is weakened by the O atom of the ether group, thus making it susceptible to abstraction and subsequent reactions. A proposed simplified reaction scheme for FEE at low temperature is shown in Fig. 16.

The activation by the ether group also provides additional sites for H atom abstractions (route (c) and (d) in Fig. 16), which then allow for other alkyl consumption reactions. In diethyl ethyl, the BDE of $C_\alpha - H$ is weakened by the adjacent O atom [45], making this site also the preferred site to have H atom abstraction reactions, followed by either O_2 addition, producing ROO radicals, or β-scission reactions.

At low to intermediate temperatures, these two reactions are competitive. ROO radicals can then undergo internal molecular isomerization form alkylhydroperoxy radicals (QOOH), which then be

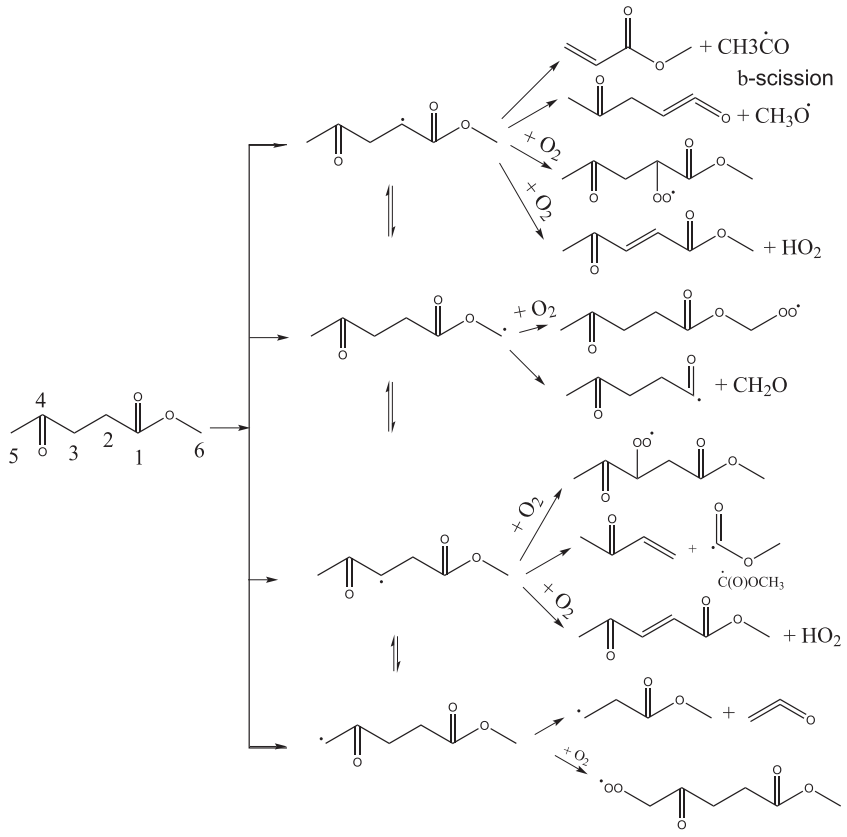

Fig. 12. Possible simplified methyl levulinate (ML) reaction scheme.

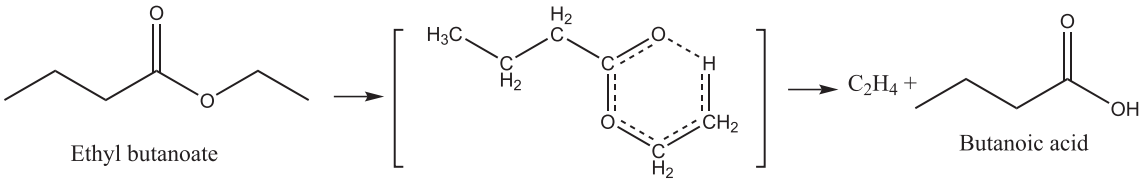

Fig. 13. Molecular elimination reaction of ethyl butanoate (EB).

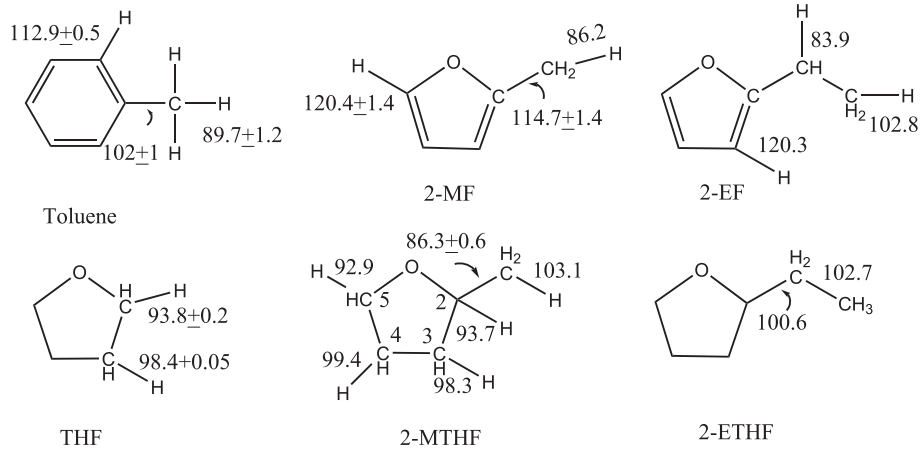

Fig. 14. Bond dissociation energy (BDE) in toluene and various cyclic ethers (data without arrow shows the BDE of nearby C–H bond) [38,40,41,39].

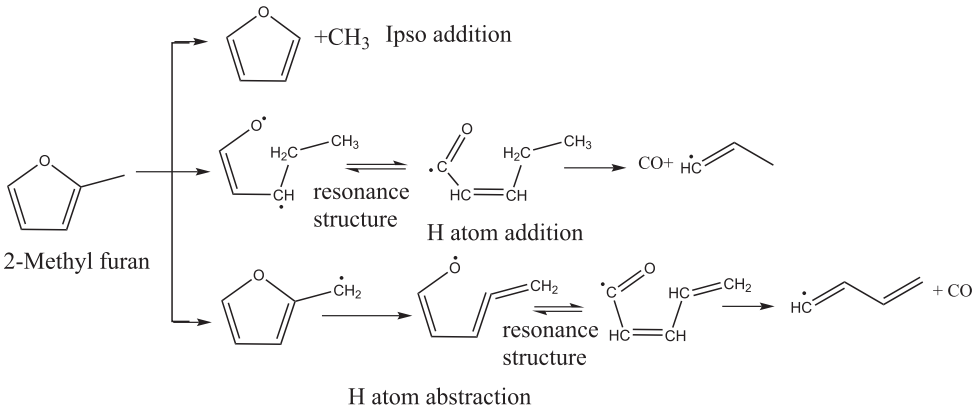

Fig. 15. Simplified reaction scheme for 2-methyl furan at low temperature [44].

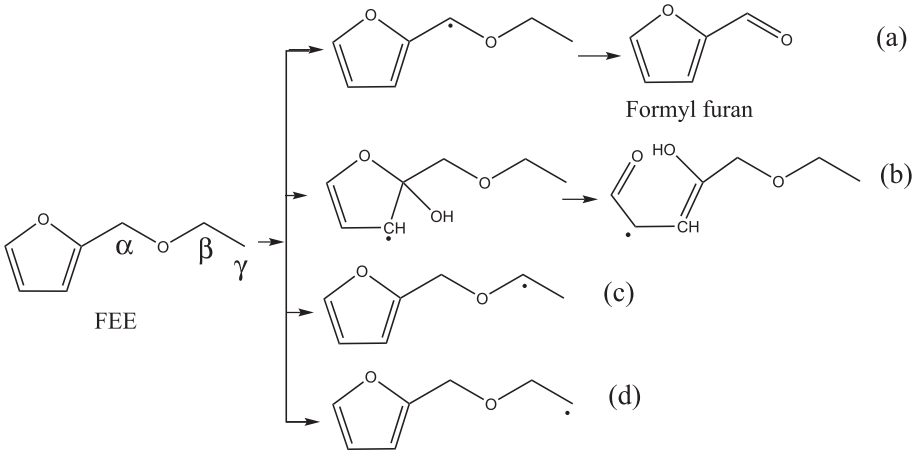

Fig. 16. Proposed reaction scheme for furfuryl ethyl ether at low temperature.

followed by low temperature branching reactions, or, alternatively, at higher temperatures, undergo β-scission [46]. The activation energies for H atom abstraction and intramolecular isomerization decrease due to the conjugation effect, i.e., the effect of the oxygen lone-pair orbital and the singly-occupied orbital at the radical-center C [45]. Thus, a straight chained ether is more reactive than its corresponding alkane. This helps to explain why FEE is more reactive than shorter chained furans.

Tetrahydrofuran (THF), like ETE, is a cyclic ether and does not contain the heteroaromatic furan ring. The name THF, though commonly used, is actually not chemically accurate. As an ether, THF has a higher DCN than furan [39]. This is mainly because the tetrahydrofuran ring is less stable. The C–H bonds on the ring are weak compared to the aromatic furan bonds (93–99 kcal/mol vs. 120 kcal/mol). This means that the ring C-H sites are the most likely sites for H atom abstraction reactions and the weak ring C–C bonds can subsequently undergo ring opening reactions via β-scission.

Substituted tetrahydrofurans, take 2-MTHF as an example, has very strong $CH_2 - H$ bonds on the substituted side chain (Fig. 14), which are much stronger than those found in aromatic furans (103 kcal/mol vs. 86.2 kcal/mol). The ring C–H bonds are weak as those in THF, and the $C_2 - H$ is weaker than others (93.7 kcal/mol). Therefore, H atom abstraction still prefers to occur at the ring H atom sites, especially at the C_2 site. The simplified reaction scheme of 2-MTHF is shown in Fig. 17 [47].

It is shown in the figure that furanyl radicals are formed after H atom abstraction, which subsequently, via β-scission, can undergo ring opening reactions, or can produce dihydrofurans. Compared to 2-MF, 2-MTHF is more readily to have ring opening reactions. This, combined with the fact that the C–H bonds on the ring are relatively weak, explains the relatively shorter ID and higher DCN (22 vs. 8.9) of 2-MTHF. [39].

Sudholt et al. [39] concluded that the side chain length has a strong influence on reaction chemistry in tetrahydrofurans, e.g., 2-butyl tetrahydrofuran has a DCN of 45.5, much higher than 2-MTHF (DCN = 22). Compared to 2-MTHF, ETE has an ethyl ether functionality on the methyl group. As discussed before, an ether group will weaken the adjacent C–H bonds, and will make the molecule more reactive than the corresponding alkyl group. Moreover, the long side chain provides more possible sites for auto-ignition reactions, resulting in a relatively high reactivity for ETE.

4. Conclusions

The objective of this paper was to investigate the anti-knock quality of sugar-derived levulinic esters (ML and EL) and cyclic ethers (FEE and ETE). To this end, combustion experiments were carried out in both an engine and a constant volume autoignition device (IQT). The results from both apparatus demonstrate that ML, EL and FEE have a higher anti-knock quality than the reference Euro95 gasoline. ETE, conversely, performed markedly worse than

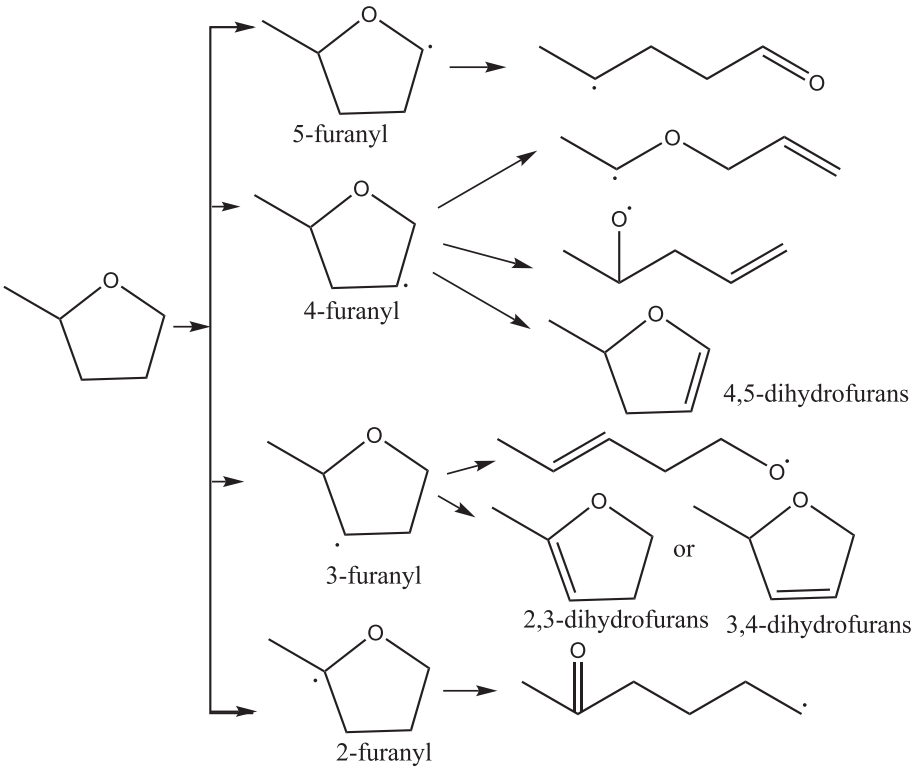

Fig. 17. Simplified reaction scheme for 2-methyltetrahydrofuran [47].

the reference fuel on both setups and might therefore be a more appropriate fuel for compression ignition engines. A chemical group additivity analysis has been performed to evaluate the impact of oxygen functionalities on DCN. Moreover, an empirical equation is presented for the relationship between distinct functionalities groups and DCN.

The main reason for the distinctions in anti-knock quality can be found in the molecular structure of the neat biofuels. ML and EL are levulinic esters, with a carbonyl group and an ester group on the carbon chain. They can readily produce stable intermediates during the auto-ignition process, thereby slowing down the overall reaction rate.

The furanic cyclic ether (FEE) has very strong ring C–H bonds. However, the saturated cyclic ether (ETE) has weak ring C–H bonds, which facilitate more readily ring opening reactions. Long side chains on the cyclic ethers further accelerate the reaction rate.

Importantly for future research, our results suggest that the modified IQT test can be used for initial screening of new fuels for their knock resistance quality and suitability as gasoline blending components.

Acknowledgments

The authors would like to thank Lisa Fouts, Earl Christensen from National Renewable Energy Laboratory – United States for their help with the experimental work. Financial support for the National Renewable Energy Laboratory employees was provided by the U.S. Department of Energy-Vehicles Technologies Office, under Contract No. DE347AC36-99GO10337 with the National Renewable Energy Laboratory. The authors also gratefully acknowledge the Chinese Scholarship Council (CSC) for the financial support. Financial support for project partners Progression Industry and Avantium was provided by AgentschapNL as part of the TKI BBE program under Contract No. TKIBE01006 (YXY-Fuels).

Appendix A

Gravimetric (Fig. 18), volumetric ISFC (Fig. 19), IMEP (Fig. 20) and thermal efficiency (Fig. 21) are plotted below as a function of the spark timing at WOT and 1500 RPM. It can be seen that the cycle-to-cycle variation is much larger than the day-to-day variation, since the calculated cycle-to-cycle variation of Euro95 is similar to other fuels, which are not shown here.

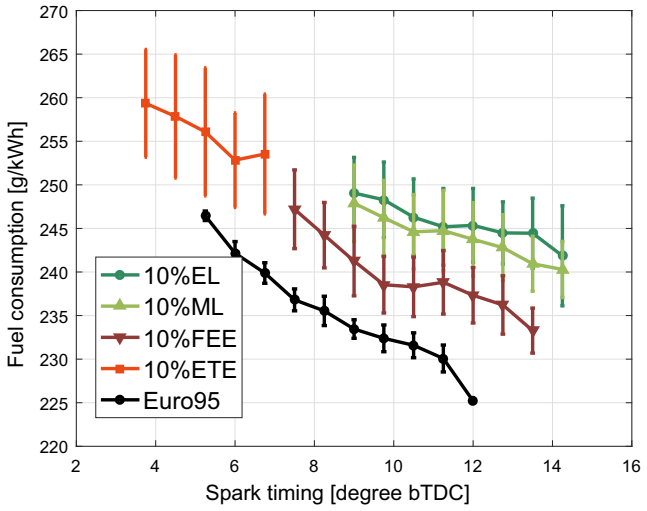

Fig. 18. Gravimetric indicated specific fuel consumption as a function of spark timing for all fuels at WOT and 1500 RPM.

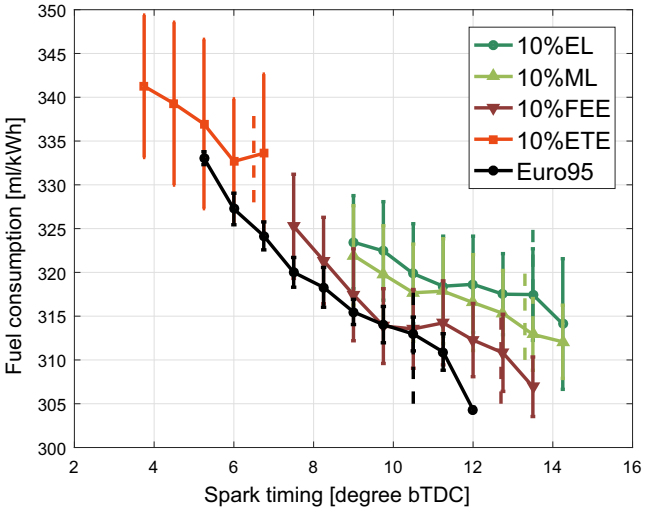

Fig. 19. Volumetric indicated specific fuel consumption as a function of spark timing for all fuels at WOT and 1500 RPM (vertical dash lines denote the KLSA points).

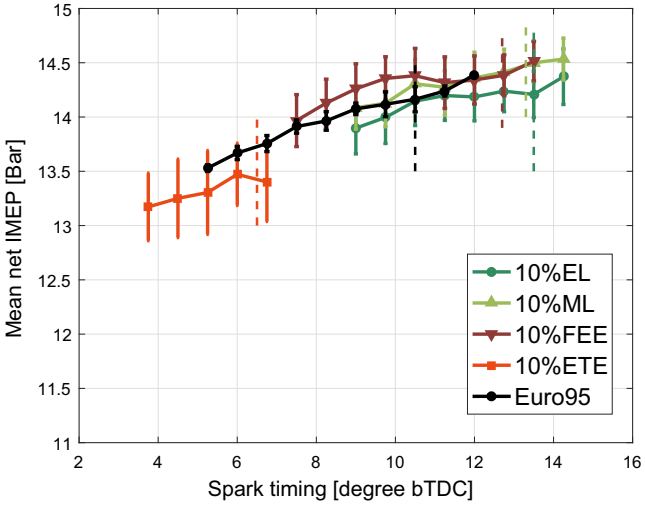

Fig. 20. IMEP as a function of spark timing for all fuels at WOT and 1500 RPM (vertical dash lines denote the KLSA points).

Appendix B. Supplementary data

Supplementary data associated with this article can be found, in the online version, at http://dx.doi.org/10.1016/j.fuel.2017.04.027.

References

[1] Huber GW, Iborra S, Corma A. Synthesis of transportation fuels from biomass: chemistry, catalysts, and engineering. Chem Rev 2006;106(9):4044–98. http://dx.doi.org/10.1021/cr068360d.
[2] Eerhart AJ, Patel MK, Faaij AP. Fuels and plastics from lignocellulosic biomass via the furan pathway: an economic analysis. Biofuels Bioprod Biorefining 2015;9(3):307–25. http://dx.doi.org/10.1002/bbb.1537.
[3] Chang C, Xu G, Zhu W, Bai J, Fang S. One-pot production of a liquid biofuel candidate–ethyl levulinate from glucose and furfural residues using a combination of extremely low sulfuric acid and zeolite USY. Fuel 2015;140:365–70. http://dx.doi.org/10.1016/j.fuel.2014.09.102.
[4] Peng L, Gao X, Chen K. Catalytic upgrading of renewable furfuryl alcohol to alkyl levulinates using $AlCl_3$ as a facile, efficient, and reusable catalyst. Fuel 2015;160:123–31. http://dx.doi.org/10.1016/j.fuel.2015.07.086.
[5] de Jong E, Gosselink RJ. Bioenergy research: advances and applications. Elsevier; 2014. http://dx.doi.org/10.1016/B978-0-444-59561-4.00017-6.

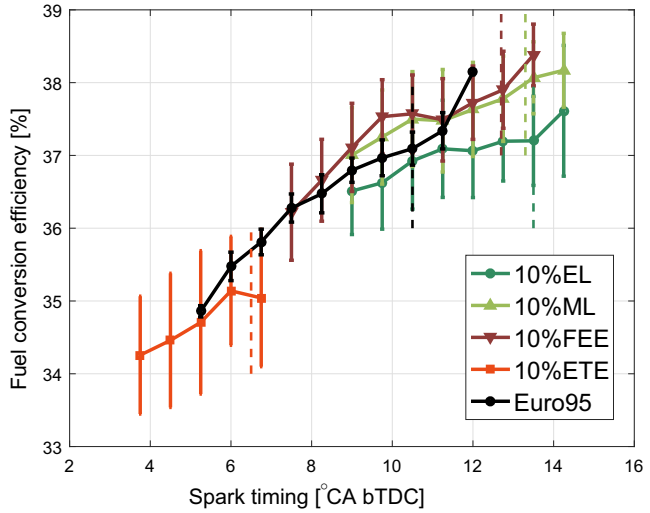

Fig. 21. Fuel conversion efficiency as a function of spark timing for all fuels at WOT and 1500 RPM (vertical dash lines denote the KLSA points).

[6] Ahmad E, Imteyaz Alam M, Pant KK, Ali Haider M. Catalytic and mechanistic insights into the production of ethyl levulinate from biorenewable feedstocks. Green Chem 2016;18(18):4789–5070. http://dx.doi.org/10.1039/c6gc01523a.
[7] de Jong E, Vijlbrief T, Hijkoop R, Gruter GJM, van der Waal JC. Promising results with YXY Diesel components in an ESC test cycle using a PACCAR Diesel engine. Biomass Bioenergy 2012;36:151–9. http://dx.doi.org/10.1016/j.biombioe.2011.10.034.
[8] van der Waal JC, de Jong E. Avantium chemicals: The high potential for the levulinic product tree. Ind Biorenewables: Pract Viewpoint A 2016:97–120.
[9] de Jong E, Dam M, Sipos L, Gruter G. Furandicarboxylic acid (FDCA), a versatile building block for a very interesting class of polyesters. Biobased Monomers Polymers Mater 2012;1105:1–13.
[10] Janssen A, Muether M, Kolbeck A, Lamping M, Pischinger S. The impact of different biofuel components in diesel blends on engine efficiency and emission performance. SAE Tech. Pap. 2010-01-2119. doi:http://dx.doi.org/10.4271/2010-01-2119.
[11] Yanowitz J, Ratcliff M, Mccormick RL, Taylor JD, Murphy MJ. Compendium of experimental cetane number data. Natl Renew Energy Lab 2014:1–48. NREL/TP-54 (August).
[12] Christensen E, Yanowitz J, Ratcliff M, McCormick RL. Renewable oxygenate blending effects on gasoline properties. Energy Fuels 2011;25:4723–33. http://dx.doi.org/10.1021/ef2010089.
[13] Kar K, Last T, Haywood C, Raine R. Measurement of vapor pressures and enthalpies of vaporization of gasoline and ethanol blends and their effects on mixture preparation in an si engine. SAE Int J Fuels Lubr 2009;1(1):132–44. http://dx.doi.org/10.4271/2008-01-0317.
[14] Lomba L, Lafuente C, García-Mardones M, Gascón I, Giner B. Thermophysical study of methyl levulinate. J Chem Thermodyn 2013;65:34–41. http://dx.doi.org/10.1016/j.jct.2013.05.025.
[15] Tian M, Van Haaren R, Reijnders J, Boot M. Lignin derivatives as potential octane boosters. SAE Int J Fuels Lubr 8 (2). doi:http://dx.doi.org/10.4271/2015-01-0963.
[16] Burgdorf K, Denbratt I. Comparison of cylinder pressure based knock detection methods. SAE Tech. Pap. 972932. doi:http://dx.doi.org/10.4271/972932.
[17] Hettinger A, Kulzer A. A new method to detect knocking zones. SAE Int J Eng 2009;2(1):645–65. http://dx.doi.org/10.4271/2009-01-0698.
[18] Bogin GE, Osecky E, Chen JY, Ratcli MA, Luecke J, Zigler BT, et al. Experiments and computational fluid dynamics modeling analysis of large n-alkane ignition kinetics in the ignition quality tester. Energy Fuels 2014;27(7):4781–94. http://dx.doi.org/10.1021/ef500769j.
[19] Bogin GE, DeFilippo A, Chen JY, Chin G, Luecke J, Ratcliff MA, et al. Numerical and experimental investigation of n-heptane autoignition in the ignition quality tester (IQT). Energy Fuels 2011;25:5562–72. http://dx.doi.org/10.1021/ef201079g.
[20] Naser N, Yang SY, Kalghatgi G, Chung SH. Relating the octane numbers of fuels to ignition delay times measured in an ignition quality tester (IQT). Fuel 2017;187:117–27. http://dx.doi.org/10.1016/j.fuel.2016.09.013.
[21] Heck SM, Pritchard HO, Griffiths JF. Cetane number vs. structure in paraffin hydrocarbons. J Chem Soc, Faraday Trans 1998;94:1725–7. http://dx.doi.org/10.1039/A800861B.
[22] Ghosh P, Jaffe SB. Detailed composition-based model for predicting the cetane number of diesel fuels. Ind Eng Chem Res 2006;45(1):346–51. http://dx.doi.org/10.1021/ie0508132.
[23] Jameel AGA, Naser N, Emwas A-H, Dooley S, Sarathy SM. Predicting fuel ignition quality using 1h nmr spectroscopy and multiple linear regression. Energy Fuels 2016. http://dx.doi.org/10.1021/acs.energyfuels.6b01690.

[24] Albahri TA. Structural group contribution method for predicting the octane number of pure hydrocarbon liquids. Ind Eng Chem Res 2003;42(3):657–62. http://dx.doi.org/10.1021/ie020306+.
[25] Ghosh P, Hickey KJ, Jaffe SB. Development of a detailed gasoline composition-based octane model. Ind Eng Chem Res 2006;45(1):337–45. http://dx.doi.org/10.1021/ie050811h.
[26] Dahmen M, Marquardt W. A novel group contribution method for the prediction of the derived cetane number of oxygenated hydrocarbons. Energy Fuels 2015;29(9):5781–801. http://dx.doi.org/10.1021/acs.energyfuels.5b01032.
[27] Dahmen M, Marquardt W. Model-based design of tailor-made biofuels. Energy Fuels 2016:1109–34. http://dx.doi.org/10.1021/acs.energyfuels.5b02674.
[28] Bogin GE, Osecky E, Ratcliff MA, Luecke J, He X, Zigler BT, Dean AM. Ignition quality tester (IQT) investigation of the negative temperature coefficient region of alkane autoignition. Energy Fuels 2013;27:1632–42. http://dx.doi.org/10.1021/ef301738b.
[29] Thion S, Zaras AM, Szöri M, Dagaut P. Theoretical kinetic study for methyl levulinate: oxidation by OH and CH_3 radicals and further unimolecular decomposition pathways. Phys Chem Chem Phys 2015;17(36):23384–91. http://dx.doi.org/10.1039/C5CP04194E.
[30] Gaïl S, Thomson M, Sarathy S, Syed S, Dagaut B, Dievart P, Marchese A, Dryer F. A wide-ranging kinetic modeling study of methyl butanoate combustion. Proc Combust Inst 2007;31:305–11.
[31] Dooley S, Curran H, Simmie J. Autoignition measurements and a validated kinetic model for the biodiesel surrogate, methyl butanoate. Combust Flame 2008;153:2–32.
[32] HadjAli K, Crochet M, Vanhove G, Ribaucour M, Minetti R. A study of the low temperature autoignition of methyl esters. Proc Combust Inst 2009;32(1):239–46. http://dx.doi.org/10.1016/j.proci.2008.09.002.
[33] Walton S, Wooldridge M, Westbrook C. An experimental investigation of structural effects on the auto-ignition properties of two C5 esters. Proc Combust Inst 2009;32(1):255–62. http://dx.doi.org/10.1016/j.proci.2008.06.208.
[34] Walton SM, Karwat DM, Teini PD, Gorny AM, Wooldridge MS. Speciation studies of methyl butanoate ignition. Fuel 2011;90(5):1796–804. http://dx.doi.org/10.1016/j.fuel.2011.01.028.
[35] Hakka MH, Bennadji H, Biet J, Yahyaoui M, Sirjean B, Warth V, et al. Oxidation of methyl and ethyl butanoates. Int J Chem Kinet 2010;42(4):226–52. http://dx.doi.org/10.1002/kin.20473.
[36] Burke U, Beeckmann J, Kopp WA, Uygun Y, Olivier H, Leonhard K, et al. A comprehensive experimental and kinetic modeling study of butanone. Combust Flame 2015;168:296–309. http://dx.doi.org/10.1016/j.combustflame.2016.03.001.
[37] El-Nahas AM, Navarro MV, Simmie JM, Bozzelli JW, Curran HJ, Dooley S, et al. Enthalpies of formation, bond dissociation energies and reaction paths for the decomposition of model biofuels: ethyl propanoate and methyl butanoate. J Phys Chem A 2007;111:3727–39. http://dx.doi.org/10.1021/jp067413s.
[38] Simmie JM, Curran HJ. Formation enthalpies and bond dissociation energies of alkylfurans. The strongest C-X bonds known? J Phys Chem A 2009;113:5128–37. http://dx.doi.org/10.1021/jp810315n.
[39] Sudholt A, Cai L, Heyne J, Haas FM, Pitsch H, Dryer FL. Ignition characteristics of a bio-derived class of saturated and unsaturated furans for engine applications. Proc Combust Inst 2015;35:2957–65. http://dx.doi.org/10.1016/j.proci.2014.06.147.
[40] Simmie JM. Kinetics and thermochemistry of 2,5-dimethyltetrahydrofuran and related oxolanes: next next-generation biofuels. J Phys Chem A 2012;116:4528–38. http://dx.doi.org/10.1021/jp301870w.
[41] Barckholtz C, Barckholtz TA, Hadad CM. C-H and N-H bond dissociation energies of small aromatic hydrocarbons. J Am Chem Soc 1999;121(2):491–500. http://dx.doi.org/10.1021/ja982454q.
[42] Thewes M, Muether M, Pischinger S, Budde M, Brunn A, Sehr A, Adomeit P, Klankermayer J. Analysis of the impact of 2-methylfuran on mixture formation and combustion in a direct-injection spark-ignition engine. Energy Fuels 2011;25(12):5549–61. http://dx.doi.org/10.1021/ef201021a.
[43] Hoppe F, Burke U, Thewes M, Heufer A, Kremer F, Pischinger S. Tailor-made fuels from biomass: potentials of 2-butanone and 2-methylfuran in direct injection spark ignition engines. Fuel 2016;167:106–17. http://dx.doi.org/10.1016/j.fuel.2015.11.039.
[44] Tran LS, Togbé C, Liu D, Felsmann D, Owald P, Glaude PA, et al. Combustion chemistry and flame structure of furan group biofuels using molecular-beam mass spectrometry and gas chromatography – Part II: 2-Methylfuran. Combust Flame 2014;161(3):766–79. http://dx.doi.org/10.1016/j.combustflame.2013.05.027.
[45] Ogura T, Miyoshi A, Koshi M. Rate coefficients of h-atom abstraction from ethers and isomerization of alkoxyalkylperoxy radicals. Phys Chem Chem Phys 2007;9(37):5133–42. http://dx.doi.org/10.1039/b706388a.
[46] Tran L-S, Pieper J, Carstensen H-H, Zhao H, Graf I, Ju Y, et al. Experimental and kinetic modeling study of diethyl ether flames. Proc Combust Inst 2016;000:1–9. http://dx.doi.org/10.1016/j.proci.2016.06.087.
[47] Moshammer K, Vranckx S, Chakravarty HK, Parab P, Fernandes RX, Kohse-Höinghaus K. An experimental and kinetic modeling study of 2-methyltetrahydrofuran flames. Combust Flame 2013;160(12):2729–43. http://dx.doi.org/10.1016/j.combustflame.2013.07.006.